# Theoretical investigations of phonon intrinsic mean-free path in zinc-blende and wurtzite AlN

A. AlShaikhi and G. P. Srivastava
*School of Physics, University of Exeter, Stocker Road, Exeter EX4 4QL, United Kingdom*
(Received 26 March 2007; revised manuscript received 14 June 2007; published 8 November 2007)

We present theoretical investigations of the anharmonic phonon mean-free path in cubic and hexagonal AlN. The cubic anharmonicity in crystal potential has been modeled within an anharmonic elastic continuum model. Numerical calculations have been carried out within the Fermi's golden rule scheme and by using the phonon dispersion and group velocity results from a full lattice dynamical model. The calculated mean-free path results for both crystal phases are compared with estimates made previously by Watari *et al.* [J. Mater. Res. **17**, 2940 (2002)] for the hexagonal phase, and a discussion on the level of agreement is provided. Our work predicts that at room temperature and above, the average phonon mean-free path for the zinc-blende phase is approximately four times that for the wurtzite phase, suggesting that AlN will exhibit far better *high thermal conductivity* behavior in its cubic phase.

DOI: 10.1103/PhysRevB.76.195205 PACS number(s): 63.20.Dj, 63.20.Kr, 65.40.−b

## I. INTRODUCTION

Due to its unique and promising properties, AlN has been the subject of numerous investigations. Among III-nitrides, AlN is regarded as a *high thermal conductivity* material,[1] with its conductivity nearly twice that of Si and comparable to that of most conductive metals.[2,3] It also exhibits excellent mechanical properties such as light weight, hardness, and corrosion resistance.[4] Being a wide band gap and high thermal conductivity material with low thermal expansion coefficient (close to that of silicon), high temperature stability, high flexure strength (equivalent to alumina), high volume resistivity, good dielectric strength, high electrical sensitivity, and low toxicity, AlN appears to be suitable for many electronic and high power applications.

Similar to other III-nitrides, AlN can be grown in two crystal phases: cubic (zinc-blende structure) and hexagonal (wurtzite structure) with nearly equal formation energy. The electronic and optical properties of the two phases of AlN are very similar.[5] The two phases are also predicted to possess similar specific heat capacity.[6] However, an examination of the phonon spectrum readily allows for making a clear distinction between the two crystal phases (see, e.g., Refs. 7 and 8). The differences in the vibrational properties of the two phases are expected to lead to corresponding differences in their thermal properties. It is thus important to examine such properties rigorously.

The thermodynamic and thermal transport properties of AlN, as a nonmetallic material, are exclusively governed by phonons. The phonon mean-free path is an important physical quantity which plays a vitally important role in determining such properties. At moderate and high temperatures, the phonon mean-free path is governed by anharmonic three-phonon scattering processes. Investigations of three-phonon relaxation processes and their temperature and frequency dependences have been largely attempted within the isotropic continuum model since the early decades of the last century.[9–12] The continuum model, however, completely ignores the role of optical phonons, as well as of phonon group velocity, in treating thermal properties of solids.

In this work, we present results for the anharmonic phonon mean-free path in cubic and hexagonal AlN using a full lattice dynamical model. A comparison of the results obtained for the two phases is provided. The role of optical phonons is also considered and discussed. We also compare our results with estimates made previously by Watari *et al.*[13] for the hexagonal phase and provide a discussion on the level of agreement. Using our results, we further comment on the high thermal conductivity behavior of AlN in the two crystal phases.

## II. THEORY AND COMPUTATIONAL DETAILS

### A. Formalism

An expression for phonon mean-free path can be derived by employing different theoretical approaches. Two standard approaches discussed in the literature[12,14] are based on the applications of (i) a variational principle and (ii) the single mode relaxation time scheme. With the application of Ziman's variational principle, the phonon mean-free path $\lambda$ can be expressed in the form

$$\lambda^{-1} = \frac{\bar{v}}{C}\sum_{\mathbf{q}s} \frac{1}{v_{\mathbf{q}s}^2}\tau_{\mathbf{q}s}^{-1} C_{\mathbf{q}s}. \tag{1}$$

Application of the single mode relaxation time approach leads to the expression

$$\lambda = \frac{\sum_{\mathbf{q}s} C_{\mathbf{q}s} v_{\mathbf{q}s} \lambda_{\mathbf{q}s}}{\bar{v}\sum_{\mathbf{q}s} C_{\mathbf{q}s}} = \frac{\sum_{\mathbf{q}s} C_{\mathbf{q}s} v_{\mathbf{q}s}^2 \tau_{\mathbf{q}s}}{\bar{v}\sum_{\mathbf{q}s} C_{\mathbf{q}s}}. \tag{2}$$

The following symbols have been used in the above equations. A phonon is identified with its wave vector $\mathbf{q}$ and its polarization index $s$; the quantities $\lambda$ and $\lambda_{\mathbf{q}s}$ are mode-average and mode-dependent phonon mean-free paths, respectively; $\tau_{\mathbf{q}s}$ represents the relaxation time of the phonon mode $\mathbf{q}s$; mode-average and mode-dependent phonon speeds are denoted by $\bar{v}$ and $v_{\mathbf{q}s}$, respectively; and $C$ and $C_{\mathbf{q}s}$ are mode-average and mode-dependent phonon specific heats, respectively, with the interrelationship

 

$$C = \sum_{\mathbf{q}s} C_{\mathbf{q}s} = \frac{\hbar^2}{k_B T^2} \sum_{\mathbf{q}s} \omega_{\mathbf{q}s}^2 \bar{n}_{\mathbf{q}s}(\bar{n}_{\mathbf{q}s}+1), \tag{3}$$

where $\hbar$ is the reduced Planck's constant, $k_B$ is Boltzmann's constant, $T$ is temperature, and $\bar{n}_{\mathbf{q}s}$ is the Bose-Einstein (i.e., equilibrium) distribution function for the mode $\mathbf{q}s$. The expression in Eq. (1) provides a lower bound to the mean-free path $\lambda$.[12] It is therefore preferable to use Eq. (2) for numerical evaluation of $\lambda$. In this work, we will therefore utilize Eq. (2).

For calculating the phonon relaxation rate $\tau_{\mathbf{q}s}^{-1}$, we have employed Fermi's golden rule formula, based on the cubic anharmonic part $V_3$ of the crystal Hamiltonian as perturbation, as described in Refs. 12 and 15. Three ingredients are required for an accurate computation of the relaxation rate: phonon dispersion relation, crystal anharmonic potential, and a numerical scheme for carrying out Brillouin zone integration. In this work, we have employed the phonon dispersion relations obtained from an adiabatic bond charge model, the crystal anhamonic potential is modeled within an anharmonic elastic continuum scheme, and the Brillouin zone integration is performed by employing an efficient special $\mathbf{q}$-point scheme. We will detail the first and third points in the next section. Here, we mention that within an anharmonic elastic continuum scheme, the cubic crystal anharmonic potential $V_3$ has been expressed as[12]

$$V_3 = \frac{1}{3!}\sqrt{\frac{\hbar^3}{8\rho^3 N_0 \Omega}} \sum_{\mathbf{q}s,\mathbf{q}'s',\mathbf{q}''s'',\mathbf{G}} \sqrt{\frac{qq'q''}{v_s v_{s'} v_{s''}}} A_{\mathbf{q}\mathbf{q}'\mathbf{q}''}^{ss's''} \delta_{\mathbf{q}+\mathbf{q}'+\mathbf{q}'',\mathbf{G}} \times (a_{\mathbf{q}s}^\dagger - a_{\mathbf{q}s})(a_{\mathbf{q}'s'}^\dagger - a_{\mathbf{q}'s'})(a_{\mathbf{q}''s''}^\dagger - a_{\mathbf{q}''s''}). \tag{4}$$

Here, $\rho$ is the material density, $N_0$ is the number of unit cells, $\Omega$ is the volume per unit cell, $\mathbf{q}$, $\mathbf{q}'$, and $\mathbf{q}''$ are the wave vectors of phonons with polarizations $s$, $s'$, and $s''$, respectively, and $a_{\mathbf{q}s}^\dagger$ ($a_{\mathbf{q}s}$) is phonon creation (annihilation) operator.

Good reviews of the theory of phonon anharmonic interaction can be found in Refs. 12, 14, 16, and 17. These reviews clearly show that it is extremely difficult, if not impossible, to calculate, from an *ab initio* theory, the three-phonon scattering strength $|A_{\mathbf{q}\mathbf{q}'\mathbf{q}''}^{ss's''}|^2$ for all required choices of the phonon vectors $\mathbf{q}$, $\mathbf{q}'$, and $\mathbf{q}''$ and polarization indices $s$, $s'$, and $s''$ needed for a full calculation of the phonon mean-free path. To the best of our knowledge, the most elaborate and workable approach to date is due to Hamilton and Parrott[18] and Srivastava.[15,19,20] Within this scheme, the crystal anharmonic potential $V_3$ is expressed by considering the crystal as an anharmonic elastic continuum, characterized by second and third order elastic constants $c_{ij}$ and $C_{ijk}$. Expressions for the scattering strengths $|A_{\mathbf{q}\mathbf{q}'\mathbf{q}''}^{ss's''}|^2$ have been derived by either restricting the three participating phonon vectors $\mathbf{q}$, $\mathbf{q}'$, and $\mathbf{q}''$ to lie in a plane[18,19] or with $\mathbf{q}$, $\mathbf{q}'$, and $\mathbf{q}''$ randomly oriented in three dimensional space.[20] In view of the fact that either $c_{ij}$ and $C_{ijk}$ are not known at all, or known with insufficient accuracy, a further level of simplification was invoked by Ziman.[14] Following the latter approach, Srivastava[12] derived the following simple expression for $|A_{\mathbf{q}\mathbf{q}'\mathbf{q}''}^{ss's''}|^2$:

$$|A_{\mathbf{q}\mathbf{q}'\mathbf{q}''}^{ss's''}|^2 = \frac{4\rho^2}{\bar{v}^2}\gamma^2 v_s^2 v_{s'}^2 v_{s''}^2, \tag{5}$$

with $v_s$, $v_{s'}$, and $v_{s''}$ as the speeds of phonons with frequencies frequencies $\omega_{\mathbf{q}s}$, $\omega_{\mathbf{q}'s'}$, and $\omega_{\mathbf{q}''s''}$, respectively, $\gamma$ as the mode-average Grüneisen's constant, and $\mathbf{G}$ as a reciprocal lattice vector. As even the mode-average $\gamma$ is not known with sufficient degree of accuracy, it is treated as a semiadjustable parameter in this work.

When dealing with anharmonic phonon interaction governed by the term $V_3$ above, it is usual to employ the concept of *single mode relaxation time*.[12,17] In this scheme, the relaxation time of a phonon mode $\mathbf{q}s$ is obtained by assuming that this mode acquires an out-of-equilibrium distribution (i.e., a displaced Bose-Einstein distribution function) while other phonon modes [i.e., $\mathbf{q}'s'$ and $\mathbf{q}''s''$ in Eq. (4)] remain in their equilibrium. Within this scheme, the relaxation rate of a phonon mode $\mathbf{q}s$ via three-phonon processes can be expressed, employing Fermi's golden rule formula, as[12]

$$\tau_{\mathbf{q}s}^{-1} = \frac{\pi\hbar\gamma^2}{\rho N_0 \Omega \bar{v}^2} \sum_{\mathbf{q}'s',\mathbf{q}''s'',\mathbf{G}} \omega_{\mathbf{q}s}\omega_{\mathbf{q}'s'}\omega_{\mathbf{q}''s''} \times \left[ \frac{\bar{n}_{\mathbf{q}'s'}(\bar{n}_{\mathbf{q}''s''}+1)}{(\bar{n}_{\mathbf{q}s}+1)} \delta(\omega_{\mathbf{q}s}+\omega_{\mathbf{q}'s'}-\omega_{\mathbf{q}''s''})\delta_{\mathbf{q}+\mathbf{q}',\mathbf{q}''+\mathbf{G}} + \frac{1}{2}\frac{\bar{n}_{\mathbf{q}'s'}\bar{n}_{\mathbf{q}''s''}}{\bar{n}_{\mathbf{q}s}} \delta(\omega_{\mathbf{q}s}-\omega_{\mathbf{q}'s'}-\omega_{\mathbf{q}''s''})\delta_{\mathbf{q}+\mathbf{G},\mathbf{q}'+\mathbf{q}''} \right]. \tag{6}$$

In the above equation, the first term represents the contribution when the mode $\mathbf{q}s$ relaxes by combining with another phonon $\mathbf{q}'s'$ to produce a third phonon $\mathbf{q}''s''$, and the second term corresponds to the mode $\mathbf{q}s$ breaking into two lower frequency phonons $\mathbf{q}'s'$ and $\mathbf{q}''s''$. Both processes are subject to energy and momentum conservation conditions via the Dirac delta function and the Kronecker delta symbol, respectively. The terms with $\mathbf{G}=0$ and $\mathbf{G}\neq 0$ are due to the so-called three-phonon normal ($N$) and umklapp ($U$) processes, respectively.

### B. Numerical procedure

In order to make numerical calculations for the two crystal phases of AlN, the summation over $\mathbf{q}''$ has been performed by using the Kronecker delta symbols, and the summation over $\mathbf{G}$ has been performed by considering eight shortest fcc reciprocal lattice vectors for the cubic phase and by considering six shortest hexagonal reciprocal lattice vectors for the wurtzite phase. For numerical calculations, we expressed the Dirac delta functions in Eq. (6) in Gaussian form using

$$\delta(x) = \lim_{\epsilon\to 0} \frac{1}{\epsilon\sqrt{\pi}} \exp\left(\frac{-x^2}{\epsilon^2}\right). \tag{7}$$

The remaining wave vector summation over $\mathbf{q}'$ has been carried out by using the concept of special wave vectors.[22,23] Accordingly, we express

$$\sum_{\mathbf{q}'} f(\mathbf{q}') = N_0 \sum_{j=1}^{N_{\mathrm{sp}}} W_j f(\mathbf{q}_j'), \tag{8}$$

where $N_{\mathrm{sp}}$ is the number of special points within the first Brillouin zone, and $W_j$ is the non-negative weight factor associated with a special point $\mathbf{q}_j'$. Numerical consideration of the momentum conservation conditions $\mathbf{q}+\mathbf{q}'\pm\mathbf{q}''=\mathbf{G}$ was made as follows:

$$|q_x + q_x' \pm q_x'' - G_x| \leq \Delta_1,$$

$$|q_y + q_y' \pm q_y'' - G_y| \leq \Delta_2,$$

$$|q_z + q_z' \pm q_z'' - G_z| \leq \Delta_3, \tag{9}$$

with $\Delta_i$ chosen as the smallest $|q_i|$ in the set of special wavevectors.

The phonon frequencies at the special wave vectors for the two phases of AlN were obtained by employing the adiabatic bond charge model.[8,21] Convergence tests were performed by considering different sets of Monkhorst-Pack special $\mathbf{q}$ points inside the Brillouin zone.[22,23] It was found that a consideration of 110 points corresponding to the $10\times10\times10$ grid for the cubic phase and 120 points corresponding to the $10\times10\times8$ grid for the hexagonal provided well converged results.

Three further considerations need to be made for numerical calculations of the mean-free path: mode phonon speeds $v_{\mathbf{q}s}$, average (acoustic) phonon speed $\bar{v}$, and the Grüneisen constant $\gamma$. The average (acoustic) phonon speed was calculated from the slopes of the acoustic phonon dispersion relation $\omega(\mathbf{q}s)$ along the principal symmetry directions for the crystal phase under consideration. For the cubic and hexagonal phases, we determined $\bar{v}^c=7.5\times10^3$ m s$^{-1}$ and $\bar{v}^h=6.77\times10^3$ m s$^{-1}$. Mode phonon speeds $v_{\mathbf{q}s}$ were calculated using three different schemes. (i) Within the isotropic continuum scheme, the speeds from the slopes of the acoustic branches were obtained as $v_{\mathrm{TA}}^c=6.75\times10^3$ m s$^{-1}$, $v_{\mathrm{LA}}^c=12.27\times10^3$ m s$^{-1}$ for the cubic phase and $v_{\mathrm{TA}}^h=6.22\times10^3$ m s$^{-1}$, $v_{\mathrm{LA}}^h=11.94\times10^3$ m s$^{-1}$ for the hexagonal phase. (ii) Mode speeds were also calculated as the phase speeds from the phonon dispersion results using $v_{\mathbf{q}s}=\omega(\mathbf{q}s)/q$. (iii) Group velocities were numerically calculated from the phonon dispersion results using $v_{\mathbf{q}s}=\nabla_{\mathbf{q}}\omega(\mathbf{q}s)$. The Grüneisen constant is mode dependent and also varies with temperature: $\gamma=\gamma(\mathbf{q}s,T)$. Keeping up with the usual practice, a mode-average $\gamma$ was considered for numerical calculations of $\lambda$. Bruls *et al.*[24] have evaluated numerical values of mode-average $\gamma$ at several temperatures in the range 90–1600 K. The values of $|\gamma|$ lie in the range 0.24–0.96. In this work, we have utilized the numerical values of $\gamma$ listed in their work.

## III. RESULTS

### A. Phonon dispersion curves

Figure 1 presents the phonon dispersion curves for *c*-AlN and *h*-AlN, obtained from the application of the adiabatic bond charge model.[8] The calculated energies and dispersion curves agree well with experiment, as discussed previously.[8] For the benefit of discussing numerical results for phonon mean-free path, we briefly point out some characteristic features of the phonon dispersion curves. In the cubic phase, there are three acoustic (ac) and three optical (op) branches. The two transverse optical (TO) branches are degenerate, with negligible dispersion, for a very large portion of the Brillouin zone. There is a negligibly small ac-op gap. The optical modes have very low group velocity (with the sixth branch with a negative group velocity) and thus are not expected to act as heat carriers, so we do not include these in the computation of average mean-free path. However, all interactions, such as ac-ac and ac-op, are taken into account.

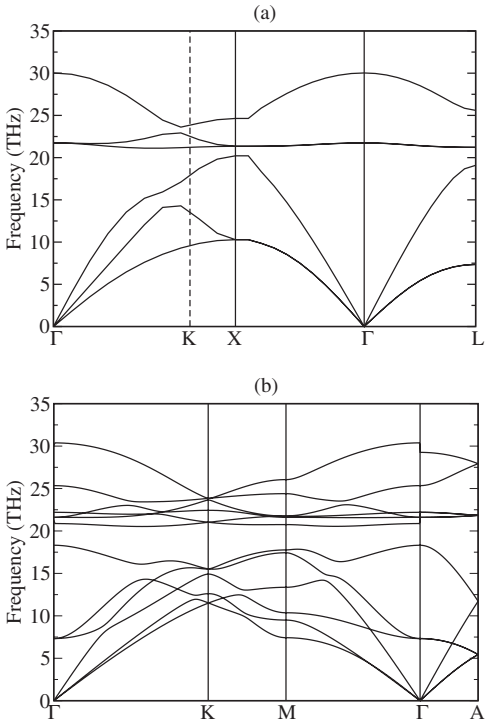


FIG. 1. Phonon dispersion curves, obtained from the adiabatic bond charge model, for (a) *c*-AlN and (b) *h*-AlN.

For the wurtzite structure, there are three acoustic, three low-lying optical, and six higher-lying optical branches. The energy gap between the lower and higher optical phonon branches is slightly larger than the ac-op gap in the cubic phase. Four optical branches (branches 7–10) show very shallow level of dispersion. The phonon group velocity in the lowest two optical branches (i.e., branches 4 and 5) is positive along the in-plane symmetry directions $\Gamma$-*K* and $\Gamma$-*M*, but is negative along the out-of-plane symmetry direction $\Gamma$-*A*. The group velocity of the third optical branch (i.e., branch 6) is negative along all the three principal symmetry directions. The next three optical branches (i.e., branches 7–10) are characterized by very low group velocity, and the last two branches (i.e., branches 11 and 12) possess negative group velocity. Thus, we have calculated the mean-free path by considering only the lowest five branches in *h*-AlN. However, all interactions, such as ac-ac and ac-op, are taken into account.

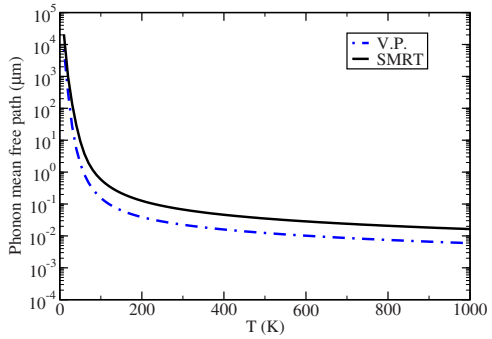


FIG. 2. (Color online) Phonon mean-free path obtained from Ziman's variational principle (dotted line) and from single mode relaxation time (SMRT) approach (solid line) in $c$-AlN. The isotropic continuum model for acoustic phonon branches was used, with $\gamma=0.8$.

### B. Comparison of results from the two theoretical approaches

In order to compare estimates from the two approaches described in Sec. II, we present in Fig. 2 the phonon anharmonic mean-free path $\lambda$ in $c$-AlN considering only acoustic branches and using the isotropic continuum model, and with a constant value of $\gamma=0.8$. As expected, the numerical estimate from the variational principle approach is lower than that obtained using the single mode relaxation time approach at all temperatures. This difference (about 67% at room temperature) arises from the fact that in Ziman's variational principle, the phonon relaxation rate is calculated using only three-phonon umklapp processes. In the rest of the work, we will, therefore, present results based on the single mode relaxation time approach.

### C. Role of group speed

Numerical results, within the single mode relaxation time scheme, for the mean-free path $\lambda$ in $c$-AlN using the three different approaches for phonon speed are shown in Fig. 3. These results were obtained by only considering the acoustic phonon branches and a constant value of $\gamma=0.8$. Although there is not much of a difference between these results at low

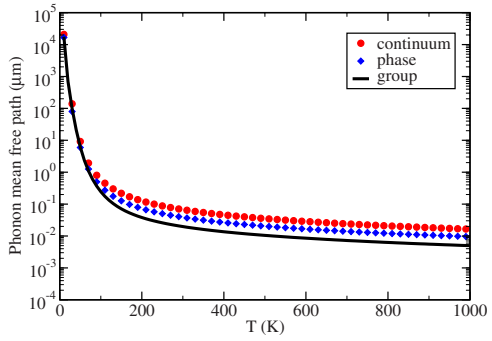


FIG. 3. (Color online) Comparison of phonon mean-free path in $c$-AlN considering acoustic modes only and using phonon continuum speed, phonon phase velocity, and phonon group velocity, with $\gamma=0.8$.

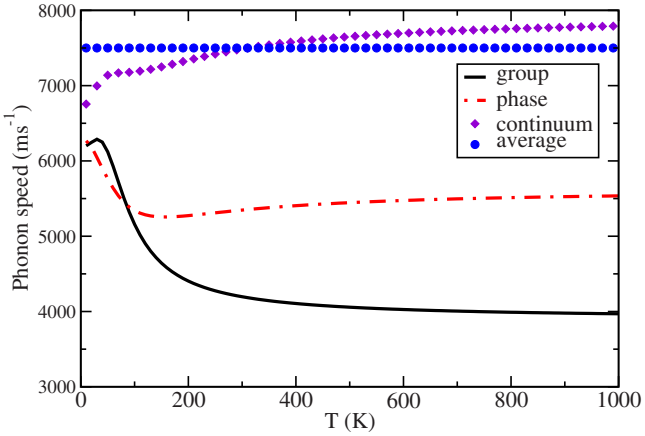


FIG. 4. (Color online) Temperature variation in $c$-AlN of population average of (i) phonon continuum speed, (ii) phonon phase speed, and (iii) phonon group speed.

temperatures, there are significant differences at temperatures above 100 K. We find that the results obtained from using the continuum mode speeds are higher than those obtained from using the phase mode speeds, which, in turn, are higher than results obtained from using group mode speeds.

These differences are justified and completely understood by examining the temperature variation, shown in Fig. 4, of the population average of the continuum, phase, and group speeds (taken over acoustic branches in the zinc-blende structure),

$$\bar{v} = \frac{\sum_{\mathbf{q}s} v_{\mathbf{q}s}\bar{n}_{\mathbf{q}s}}{\sum_{\mathbf{q}s} \bar{n}_{\mathbf{q}s}}. \tag{10}$$

It can be seen that above 100 K, the population averaged phonon continuum speed is higher than the phase speed, which, in turn, is higher than the group speed. This is because at low temperatures, most of the excited phonons in solids are confined to low-$q$ or long-wavelength acoustic branches. These phonons have high group speeds. However, with increase in temperature, more phonons from higher branches (which have lower, and in some cases negligible or negative, group velocities) are excited. In this sense, the phonon population average group speed will drop dramatically with increase of temperature. Above a certain temperature, when phonons from all branches have been populated, there will be no appreciable drop or change in the population average speed.

The differences discussed above clearly establish the importance of using numerically accurate phonon group speed in the calculation of anharmonic mean-free path and related thermal properties. All the results discussed in further sections are based on the use of mode group speeds.

### D. Role of normal and umklapp processes

In order to discuss the relative roles of three-phonon normal and umklapp processes in controlling phonon mean-free

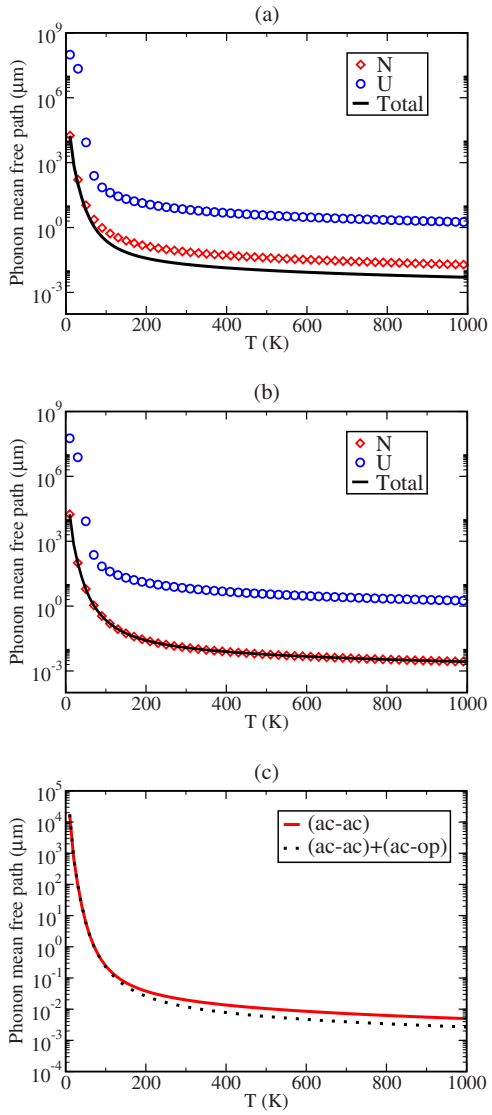


FIG. 5. (Color online) Contributions to the acoustic phonon mean-free path in $c$-AlN from normal and umklapp processes, with $\gamma$=0.8. Panel (a) shows $N$ and $U$ contributions for ac-ac interactions. Panel (b) shows $N$ and $U$ contributions with ac-ac and ac-op interactions. Panel (c) presents a comparison of total results with and without ac-op interactions.

path, we carried out calculations for umklapp processes by including the set of shortest **G** vectors. Inclusion of the set of second smallest **G** vectors decreases λ by approximately 6%, 12%, and 16% at 100, 300, and 1000 K, respectively, for $c$-AlN. The results presented henceforth were carried out by including the set of shortest **G** vectors.

Figure 5(a) shows contributions toward the acoustic phonon mean-free path from three-phonon normal and umklapp processes. The calculations were performed for $c$-AlN by only considering acoustic phonon branches, numerical group velocities, and $\gamma$=0.8 as a constant value for Grüneisen's constant. The phonon mean-free path due to umklapp processes is much larger than the contribution from normal processes at all temperatures considered here. This reveals that phonon-phonon interactions are dominated by normal processes. This conclusion contrasts with the results obtained using the (simpler) isotropic continuum model,[12,15,20] which indicates that umklapp processes (treated within an artificial grafting scheme) are at least as strong as normal processes. We also point out that our result contrasts many other previous works in the field of phonon-phonon interactions, which only consider umklapp processes (and thus completely ignore normal processes).[25–27]

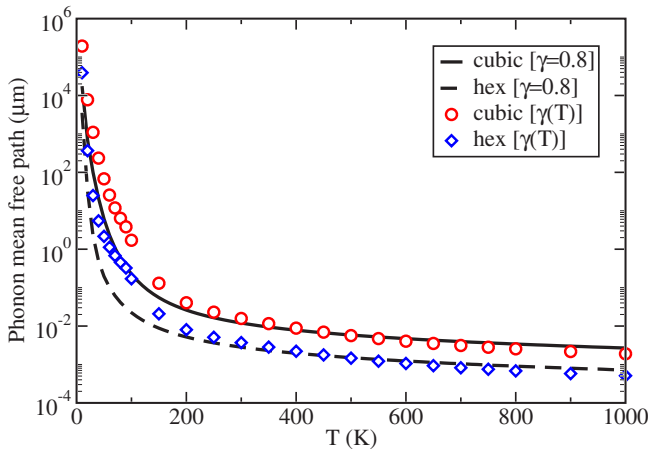


FIG. 6. (Color online) Mean-free path of (i) acoustic phonons in $c$-AlN and (ii) phonons in the lowest five branches in $h$-AlN. Results are presented with and without temperature dependence of Grüneisen constant $\gamma$. The effect of $\gamma(T)$, taken from the work of Bruls *et al.* (Ref. 24), can be clearly seen.

### E. Effect of acoustic-optical interaction in $c$-AlN

The consideration of acoustic-optical (ac-op) interactions in $c$-AlN, as shown in Fig. 5(b), reduces acoustic phonon mean-free path due to both $N$ and $U$ processes. While the acoustic mean-free path due to normal processes is reduced by about 68% at 100 K and by about 86% at 1000 K, the acoustic mean-free path due to umklapp processes is reduced by about 3% only at 100 K and by less than 2% at 1000 K. The results displayed in Fig. 5(c) show a comparison of the average phonon mean-free path of acoustic phonons (including both normal and umklapp contributions) with and without the consideration of optical modes in $c$-AlN. The inclusion of the acoustic-optical interactions in the calculations results in reducing the acoustic phonon mean-free path at all temperatures. While this reduction is very small at low temperatures, it reaches around 39% at room temperature and 46% at 1000 K.

### F. Crystal phase dependence

Results displayed in Fig. 6 show a comparison between the theoretical results for the average phonon mean-free path of acoustic modes (i) in $c$-AlN and (ii) in $h$-AlN (considering the lowest five phonon branches—modes with positive group velocity). The results include interactions of these phonon modes with acoustic as well as optical modes. The results were obtained by using a constant value for the Grüneisen constant: $\gamma$=0.8. As expected, the phonon mean-free path in

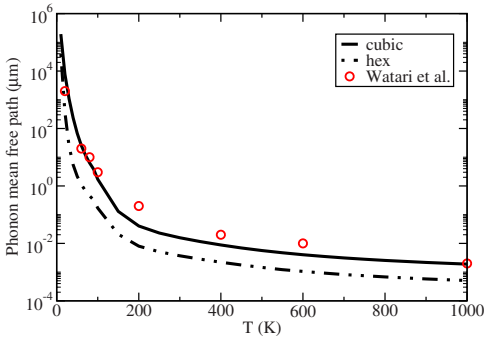


FIG. 7. (Color online) Mean-free path of (i) acoustic phonons in *c*-AlN considering ac-op interactions taking $\gamma(T)$ presented in Ref. 24 and (ii) lowest five phonon branches in *h*-AlN considering their interactions with phonons in all higher branches taking $\gamma(T)$ presented in Ref. 24. Circles show estimates made by Watari *et al.* (Ref. 13).

*h*-AlN is lower than that in *c*-AlN at all temperatures. At room temperature and above, the mean-free path in *c*-AlN is obtained to be nearly four times that in *h*-AlN. We also find that this ratio can be affected by the temperature dependence of $\gamma$. In the figure, we also show the results obtained by utilizing $\gamma(T)$ as tabulated in the work by Bruls *et al.*[24] We note that there are no data available in the work of Bruls *et al.* below 90 K. We have discarded the (very small) value of $\gamma$ at 100 K in their table, and for temperatures below 90 K, we have adopted the value at 90 K. The effect is that a much bigger difference in the mean-free path is obtained at low temperatures than at high temperatures. Still, at room temperature and above, the mean-free path in *c*-AlN remains approximately four times that in *h*-AlN.

### G. Comparison with previous results

Watari *et al.*[13] calculated the average anharmonic phonon mean-free path $\lambda$ from the relation $\lambda = 3\kappa/\bar{v}C$ and using the prediction by Slack *et al.*[2] of the intrinsic thermal conductivity $\kappa$ of AlN in the wurtzite phase by correcting the residual oxygen content in a high-purity single crystal. It is worth emphasizing that the results obtained in Ref. 2 for the conductivity are primarily for heat flow along the *c* axis of the wurtzite structure. The difference between conductivity values parallel and perpendicular to the *c* axis is estimated to be approximately 20% at low temperatures and approximately 5% at room temperature and above. These points should be kept in mind when discussing comparison of our results with those of Watari *et al.* for the anharmonic mean-free path.

In Fig. 7, we have compared our calculated results for both *c*-AlN and *h*-AlN with the estimates made by Watari *et al.* As mentioned earlier, we have used the mode-average $\gamma(T)$ as presented in the work of Bruls *et al.* Our results for the cubic phase appear to be in reasonable agreement with the results obtained by Watari *et al.* However, in view of the points made in the previous paragraph, such a comparison should be made with caution. All that can be said with some degree of confidence is that both this work as well as the work by Watari *et al.* have obtained similar temperature variation of the mean-free path over a large temperature range.

### H. Implication for high thermal conductivity behavior

Using the expression $\kappa = \frac{1}{3}C\bar{v}\lambda$, based on the consideration of three acoustic branches in the cubic phase and the lowest five branches in the hexagonal phase (ignoring the sixth branch on account of very small group speed), from our numerical work at high temperatures (i.e., using $\bar{n}_{\mathbf{q}s} = \frac{k_B T}{\hbar\omega_{\mathbf{q}s}}$), we find that the lattice thermal conductivity ($\kappa$) of *c*-AlN will be approximately 2.7 times that of *h*-AlN at room temperature and above, where anharmonicity provides the main source of phonon scattering. This estimated ratio, based on the assumption that the mode-average Grüneisen's constant $\gamma$ is the same for both the crystalline phases, should be taken as an upper limit, and a full-scale calculation must be performed to obtain an accurate value at a given temperature. This result clearly suggests that AlN would be a far better high thermal conductivity material when grown in its cubic phase than in its hexagonal phase.

Our prediction for the relative high thermal conductivity behaviors of the cubic and hexagonal phases of AlN can be compared with the prediction obtained from a simple theory presented by Morelli and Slack[28] and detailed by Slack.[29] This theory uses a simple counting scheme (to account for conductivity contribution from each basis atom in the unit cell) and a scaling scheme for adjusting the Debye radius for a complex structure with several atoms per unit cell. According to their theory, the thermal conductivity of a complex crystal structure (such as the wurtzite structure) near the Debye temperature can be expressed as

$$\kappa = A\frac{\bar{M}\theta^3\delta}{\gamma^2 T n^{2/3}},$$

where $A$ is an appropriate constant, $\bar{M}$ is average atomic mass, $\theta$ is the Debye temperature, $\delta^3$ is atomic volume, and $n$ is the number of basis atoms per unit cell.

In agreement with our work, the Morelli-Slack theory predicts that the thermal conductivity of the cubic phase is higher than that of the hexagonal phase. However, the Morelli-Slack theory predicts that at high temperatures, the conductivity of the cubic phase will be 1.59 ($=2^{3/2}$) times that of the hexagonal phase. This ratio is quite small compared to our (more accurate) prediction of approximately 2.7. This difference mainly arises due to the two main simplifications involved in the Morelli-Slack theory. In particular, their theory is based on the application of the linear dispersion relation $\omega_{\mathbf{q}s} = \bar{v}q$ within the isotropic continuum limit and the corresponding quadratic frequency variation of the density of states $g(\omega) \propto \omega^2$ for all phonon modes. Figure 1 in this work clearly demonstrates that the linear dispersion relation is not justified for all modes, particularly for the non-cubic wurtzite structure.

There are two main reasons why the thermal conductivity of the cubic AlN would be higher than that of the hexagonal AlN. The first is that the cubic phase represents a simpler crystal structure with fewer number of optical phonon

branches than the hexagonal phase, as mentioned in Sec. III A. The presence of nine optical branches in the hexagonal phase leads to much stronger phonon-phonon interaction compared to the cubic phase which contains only three optical branches. The second reason is that the average phonon speed in the hexagonal phase is somewhat smaller than in the cubic phase. A combination of these two factors makes both the mean-free path (MFP) and the conductivity (which is proportional to the product of MFP and average speed) of the cubic phase larger than that of the hexagonal phase. This comparative result is not only limited to AlN but is valid for all materials that can adopt two or more energetically-competing crystalline phases, such as other III-nitrides.

The main ingredient of this work, viz., the anharmonic phonon relaxation rate, can be utilized to develop a full-scale computational method for studying thermal conductivity of crystalline materials. In particular, it would be highly beneficial to provide accurate, parameter-free comparative estimates of the conductivity of the cubic and hexagonal phases of III-nitrides. This would help explain existing experimental results for bulk nitrides.[30] In addition, such a theoretical development would help provide a clearer understanding, than is currently possible from theories based on the continuum model, of conductivity results for nitride alloys[31] and nitride thin films[32] based on clearer physical considerations.

## IV. SUMMARY

We have theoretically investigated the phonon anharmonic mean-free path in cubic and hexagonal AlN. The method employed the Fermi's golden rule formula and the calculations were performed using (i) phonon dispersion relations obtained from the application of the adiabatic bond charge model, (ii) cubic anharmonic crystal potential derived within an anharmonic elastic continuum model, (iii) mode-average and temperature dependent Grüneisen constant, and (iv) a special **q**-point scheme for Brillouin zone summation. Our results can be summarized as follows.

(1) Three-phonon normal processes dominate the phonon relaxation rate and thus heavily control the mean-free path.

(2) Assuming that mode-average $\gamma$ is the same for cubic and hexagonal crystal phases, our work predicts that the phonon mean-free path for *c*-AlN is approximately four times that for *h*-AlN at room temperature and above. In particular, the mean-free path of acoustic phonons in *c*-AlN ranges from 2 nm at 1000 K to approximately 2000 nm at low temperatures, while the mean-free path of phonons (including acoustic and low-lying optical modes with positive group velocity) in *h*-AlN ranges from 0.5 nm at 1000 K to 200 nm at low temperatures.

(3) Our work suggests that AlN will exhibit a far improved high thermal conductivity behavior (up to a maximum of 2.7 times) in its cubic phase compared to its hexagonal phase at room temperature and above.

## ACKNOWLEDGMENT

A. A. gratefully acknowledges financial support from the King Abdul Aziz University, Saudi Arabia.

[1] S. L. Shinde and J. S. Goel, *High Thermal Conductivity Materials* (Springer, New York, 2006).
[2] G. A. Slack, R. A. Tanzilli, R. O. Pohl, and J. W. Vandersande, J. Phys. Chem. Solids **48**, 641 (1987).
[3] J. C. Nipko and C. K. Loong, Phys. Rev. B **57**, 10550 (1998).
[4] M. E. Levinshtein, S. L. Rumyantsev, and M. S. Shur, *Properties of Advanced Semiconductor Materials: GaN, AlN, InN, BN, SiC, SiGe* (Wiley, New York, 2001).
[5] F. Litimein, B. Bouhafs, Z. Dridi, and P. Ruterana, New J. Phys. **4**, 1 (2002).
[6] A. AlShaikhi and G. P. Srivastava, Phys. Status Solidi C **3**, 1495 (2006).
[7] H. Siegle, G. Kaczmarczyk, L. Filippidis, A. P. Litvinchuk, A. Hoffmann, and C. Thomsen, Phys. Rev. B **55**, 7000 (1997).
[8] H. M. Tütüncü and G. P. Srivastava, Phys. Rev. B **62**, 5028 (2000).
[9] R. Peierls, Ann. Phys. **3**, 1055 (1929).
[10] C. Herring, Phys. Rev. B **95**, 954 (1954).
[11] G. L. Guthrie, Phys. Rev. B **152**, 801 (1966).
[12] G. P. Srivastava, *The Physics of Phonons* (Hilger, Bristol 1990).
[13] K. Watari, H. Nakano, K. Urabe, K. Ishizaki, S. Cao, and K. Mori, J. Mater. Res. **17**, 2940 (2002).
[14] J. M. Ziman, *Electrons and Phonons* (Oxford University Press, New York, 1967).
[15] G. P. Srivastava, Pramana **3**, 209 (1974); **6**, 1 (1976); Philos. Mag. **34**, 795 (1976).
[16] G. Liebfried, *Handbunch der Physik*, 2nd ed. (Springer-Verlag, Berlin, 1955), Vol. 7-1, especially p. 290 ff.
[17] P. Carruthers, Rev. Mod. Phys. **33**, 92 (1961).
[18] R. A. H. Hamilton and J. E. Parrot, Phys. Rev. **178**, 1284 (1969).
[19] G. P. Srivastava, D. P. Singh, and G. S. Verma, Phys. Rev. B **6**, 3053 (1972).
[20] G. P. Srivastava, J. Phys. Chem. Solids **41**, 357 (1980).
[21] W. Weber, Phys. Rev. B **15**, 4789 (1977).
[22] H. J. Monkhorst and J. D. Pack, Phys. Rev. B **13**, 5188 (1976).
[23] G. P. Srivastava, *Theoretical Modelling of Semiconductor Surfaces* (World Scientific, Singapore, 1999).
[24] R. J. Bruls, H. T. Hintzen, G. de With, R. Metselaar, and J. C. van Miltenburg, J. Phys. Chem. Solids **62**, 783 (2001).
[25] Y.-J. Han, Phys. Rev. B **54**, 8977 (1996).
[26] A. Balandin and K. L. Wang, Phys. Rev. B **58**, 1544 (1998).
[27] Y. Xiao, X. H. Yan, J. X. Cao, and J. W. Ding, J. Phys.: Condens. Matter **15**, 341 (2003).
[28] D. T. Morelli and G. A. Slack, in *High Thermal Conductivity Materials*, edited by S. L. Shinde and J. S. Goel (Springer, New York, 2006).
[29] G. A. Slack, Solid State Phys. **34**, 1 (1979).
[30] W. Liu and A. A. Balandin, J. Appl. Phys. **97**, 073710 (2005), and references therein.
[31] W. Liu and A. A. Balandin, Appl. Phys. Lett. **85**, 5230 (2004).
[32] J. Zou, D. Kotchetkov, and A. A. Balandin, J. Appl. Phys. **92**, 2534 (2002); B. C. Daly, H. J. Maris, A. V. Nurmikko, M. Kubal, and J. Han, *ibid.* **92**, 3820 (2002).